Salidroside ameliorates lipopolysaccharide-induced ferroptosis in chondrocytes via regulation of the sirt1/foxo1 axis

XU ZHANG[1,2], LING HUANG[3], WENJUN FENG[4], DANGHAN XU[4] and YIRONG ZENG[4]

[1]1st School of Medicine, Guangzhou University of Chinese Medicine, Guangzhou, Guangdong 510405, P.R. China; [2]Department of Orthopedics, Leliu Hospital Affiliated to Shunde Hospital of Guangzhou University of Chinese Medicine, Guangzhou, Guangdong 528000, P.R. China; [3]Department of Orthopedics, Shunde Third People's Hospital, Guangzhou, Guangdong 528000, P.R. China; [4]Department of Orthopaedics, First Affiliated Hospital, Guangzhou University of Chinese Medicine, Guangzhou, Guangdong 510405, P.R. China

Received October 23, 2024; Accepted February 18, 2025

DOI: 10.3892/mmr.2025.13502

Abstract. Salidroside (SAL) is a bioactive constituent extracted from *Rhodiola rosea* plant and exerts antioxidant and anti-inflammatory properties. However, understanding of SAL for the treatment of arthritis is limited. The aim of the present study was to investigate whether SAL treats lipopolysaccharide (LPS)-induced chondrocyte injury by modulating the sirt1 silent information regulator 1)/FoxO1 (forkhead transcription factors O1) signaling pathway. Network pharmacology was used to screen the potential pathway of SAL for the treatment of osteoarthritis via the ferroptosis pathway. Subsequently, a chondrocyte inflammation model was established *in vitro* using LPS and SAL was used as a drug treatment. Effects of SAL treatment of chondrocytes was evaluated by western blot analysis, fluorescence, cell viability and oxidative assay. Analysis revealed that SAL significantly attenuated LPS-induced apoptosis and accumulation of oxides in chondrocytes, thereby protecting the integrity of cartilage extracellular matrix. In addition, SAL promoted the activation of the sirt1/foxo1 signaling cascade, which alleviated LPS-induced ferroptosis in chondrocytes. The present study demonstrated that SAL attenuated LPS-induced chondrocyte ferroptosis by regulating the sirt1/foxo1 pathway. This may provide a potential therapeutic avenue for cartilage damage in osteoarthritis.

Introduction

Osteoarthritis (OA) is one of the most common degenerative bone and joint diseases among the elderly, characterized by joint pain and transient morning stiffness, accompanied by joint swelling, tenderness and joint movement noise, and in severe cases, joint deformity. OA affects ~10% of males and ~18% of females aged >60 years worldwide (1). In developed countries, the economic loss due to OA accounts for 1.0-2.5% of the gross domestic product and it is one of the notable sources of pain, disability and socio-economic cost in the world (2). In the rapidly aging population, OA is a serious health problem.

FoxO1 forkhead transcription factors O1 (FoxO1), a member of the mammalian FoxO family, is expressed in almost all tissue in all mammals and has an important role in the regulation of apoptosis and oxidative stress (3). Akasaki *et al* (4) revealed that FoxO1 expression in chondrocytes from patients with OA is considerably reduced compared with that in chondrocytes from healthy individuals (4). Matsuzaki *et al* (5) revealed that overexpression of FoxO1 in OA chondrocytes decreases inflammatory mediators and cartilage-degrading enzymes and increases the expression of protective genes, whereas FoxO1 knockout mice exhibit a markedly increased onset of OA (5). Silent information regulator 1 (Sirt1) is a NAD^+-dependent histone deacetylase, a key target for the treatment of numerous types of metabolic disorder (such as type 2 diabetes mellitus) and a longevity gene. Sirt1 factors are involved in the regulation of various signaling pathways such as P53 and Sitr1 (6). In the Sirt1/FoxO1 signaling pathway, Sirt1 serves a role in controlling the nuclear translocation and transcriptional activity of FoxO1, and positively or negatively regulates the activity of FoxO1 according to the target gene or cell type. With the in-depth study of signaling pathways, the association between FoxO1 and Sirt1 has been demonstrated in several diseases, such as diabetic nephropathy, depression, hypertension and OA (7-10). Sirt1/FoxO1 signaling pathway may have therapeutic potential as it regulates cellular ferroptosis in cardiovascular and neurological disease (11,12). However, the roles of ferroptosis and the Sirt1/FoxO1 signaling pathway in OA remain unclear and require further validation.

Salidroside (SAL) is the bioactive constituent extracted from the *Rhodiola rosea* plant, which exhibits pharmacological properties. These include anti-hypoxic, anti-inflammatory

Correspondence to: Professor Yirong Zeng, Department of Orthopaedics, First Affiliated Hospital, Guangzhou University of Chinese Medicine, 16 Jichang Road, Baiyun, Guangzhou, Guangdong 510405, P.R. China
E-mail: z39298@sohu.com

Key words: salidroside, osteoarthritis, sirt1/foxo1 signaling, ferroptosis

and anti-fibrotic effects, as well as the ability to increase the effectiveness of the immune system and safeguard the nervous system. It has also been established as being safe and lacking toxicity (13). Extensive research has demonstrated the beneficial anti-inflammatory impact of SAL on various body systems, including the nervous (14), digestive (15) and circulatory systems (16), with notable effects on joint inflammation as well (17). SAL has been documented to offer protection against cartilage degeneration, exhibiting promising therapeutic effects against the early acute phase symptoms of OA in rats (18,19). However, the precise mechanism by which SAL influences the regulation of chondrocyte ferroptosis through the Sirt1/FoxO1 pathway in the treatment of OA remains to be elucidated.

The aim of the present study was to verify whether SAL could reduce chondrocyte apoptosis and oxidative stress and treat osteoarthritis through the Sirt1/FoxO1 pathway by bioinformatics analysis and *in vitro* experiments.

Materials and methods

Databases, analysis platforms and software. Drug target prediction (targetnet; targetnet.scbdd.com/) was used for SAL target acquisition. Drug target prediction (SwissTargetPrediction; http://swisstargetprediction.ch/) is used for SAL target acquisition. Drug target prediction (Pharmmapper; pharmmapper. com/) is used for SAL target acquisition. Online Catalog of Human Genetic Diseases (OMIM; omim.org/) for Osteoarthritis Disease Target Acquisition. Human Gene Database (GeneCards; genecards.org) for Osteoarthritis Disease Target Acquisition. ferroptosis Database (FerrDb; zhounan.org/ferrdb/current/) for access to ferroptosis-related targets. UniProt protein database (uniprot.org) was used to match the protein target information obtained and corrected to uniform gene names. STRING database (string-db.org) PPI network construction and core target screening. Metascape database (metascape.org) for Gene ontology (GO) functional enrichment analysis and Kyoto encyclopedia of genes and genomes (KEGG) pathway enrichment analysis. Cytoscape 3.9.1 software (https://Cytoscape.org) building 'target-pathway' networks. Microbiotics Analysis Platform (bioinformatics.com.cn) visualizes the results of the enrichment analysis.

SAL target acquisition. Chemical structure formula was obtained from PubChem and entered into target prediction websites Targenet, SwissTargetPrediction and Pharmmapper, to obtain the predicted target. The chemical compositions and corresponding target proteins were exported. Non-corresponding target compositions were eliminated, and information was entered into a Microsoft Excel(Office16, Microsoft Corp.) spreadsheet. Due to the inconsistency of gene name codes in different databases, target names were standardized before analysis and the parameter values were set to 'reviewed, human' and 'gene name primary' in the UniProt protein database. The verified human protein target file was downloaded after setting 'reviewed, human' and 'gene name primary' parameters in the UniProt protein database and protein targets were matched with the protein information in the UniProt database and corrected to a unified gene symbol.

Disease target acquisition. GeneCards, DrugBank and Therapeutic Target Database (TTD) databases were searched for potential therapeutic targets for OA using 'osteoarthritis' as the key word. Targets were combined, and duplicate genes were removed to create a target set.

Potential ferroptosis pathway targets of action for SAL in the treatment of OA. To determine the mechanism of interaction of SAL in the intervention and treatment of OA, known ferroptosis-associated targets were downloaded from the FerrDb database; following Wein mapping, the intersection of SAL targets of action, OA targets and ferroptosis targets, was visualized as a Venn diagram (Venny 2.1.0 - CSIC; bioinfogp.cnb.csic.es/tools/venny/).

Construction of protein-protein interaction (PPI) network and screening of core targets. All intersecting targets were imported into the STRING database and then a PPI network model was constructed. The PPI network modeling diagram enables the visualization of the cellular functional interactions between cellular expression and function of proteins. After obtaining the search results, the PPI network diagram was imported into Cytoscape 3.9.1 software (xiazai.zol.com.cn/detail/53/528431.shtml)to analyze the topological parameters of each node using the plug-in CytoNCA and evaluate the importance of targets in the network from three screening dimensions (node connectivity, median centrality and proximity to centrality) and ultimately construct a core target screening network to obtain core targets.

Core target Gene Ontology (GO) biofunction and Kyoto Encyclopedia of Genes and Genomes (KEGG) information transduction pathway enrichment analysis. To determine gene functions and their involvement in signaling pathways for the key targets, these targets were integrated into the Metascape database. The genes underwent GO (20) functional and KEGG (21) pathway enrichment analysis. The outcomes were visualized using MBC platform (bioinformatics.com.cn/). The visualization was organized by P-value, with the first 10 entries of each section of the GO and the KEGG analysis displayed through the MBC platform. To elucidate the interconnections between the targets and pathways, a 'target-pathway' network was established using Cytoscape 3.9.1 software for the top 20 signaling pathways and the genes that modulate them, providing a clearer understanding of the regulatory association.

Reagents and materials. Penicillin/streptomycin, fetal bovine serum (FBS; Solarbio Science & Technology Co., Ltd.) and trypsin were purchased from Thermo Fisher Scientific, Inc. DMEM/F12 and PBS were purchased from Wuhan Servicebio Technology Co., Ltd. Cell Counting Kit-8 (CCK-8) was purchased from GLPBIO Technology LLC. RIPA lysis and loading buffer BCA analysis and DS-PAGE gel preparation kit were provided by Beyotime Biotechnology. Toluidine blue staining (cat. no. G3660) and glutathione (GSH, cat. no. BC1175) and malondialdehyde (MDA, cat. no. BC0025) content assay kit were purchased from Beijing Solarbio Science & Technology Co., Ltd. Nicotinamide was purchased from sigma

(cat. no. 38806381). Collagen II (Col2; cat. no. AF0135), MMP3 (cat. no. AF0217), MMP13 (cat. no. AF5355), Bax (cat. no. AF0120), Bcl2 (cat. no. AF6139), Gpx4 (Glutathione Peroxidase 4, cat. no. DF6701), SLC7A11 (cat. no. DF12509), Sirt1 (cat. no. DF6033), FoxO1 (cat. no. AF3419), β-actin (cat. no. AF7018) and goat anti-rabbit IgG (cat. no. S0001) were purchased from Affinity Biosciences.

Primary cell extraction and culture. This animal experiment was approved by the Animal Ethics Committee of the First Affiliated Hospital of Guangzhou University of Traditional Chinese Medicine (approval no. GZTCMF1-20240301-3). Chondrocytes were harvested from 1-week-old C57BL/6J mice (22,23). In total, we extracted 4 male mice, and their average weight was about 6 g. The animals were humanely euthanized via cervical dislocation, and death was confirmed by cardiac arrest, followed by full-body disinfection with alcohol. The lower limbs were excised and the knee joints were extracted. The articular cartilage was sectioned into 1 cm^3 pieces. These cartilage fragments were initially treated with 0.25% trypsin for 30 min at 37˚C to dissociate the cells and digested with 0.25% type II collagenase (Sigma-Aldrich; Merck KGaA; cat. no. 9001121) for 6 h at 37˚C temperature to degrade the extracellular matrix. The resulting cell suspension was filtered to purify the chondrocytes, as previously descried (24). The isolated chondrocytes were cultured in DMEM/F12 enriched with 10% FBS at 37˚C and 5% CO_2. When cells reached 80% confluence, they were passaged. For subsequent experimental procedures, chondrocytes from the second to fifth passage were used.

CCK-8 assay. Chondrocytes were seeded into 96-well plates at a density of ≥5,000 cells/well. Once the cells had adhered, they were challenged with LPS at a concentration of 1 μg/ml. Cells were exposed to a series of SAL concentrations (0.0, 1.0, 2.5, 5.0, 10.0, 25.0 and 50.0 μM) in a stepwise manner at 37˚C. After 24 or 48 h, the culture medium was removed, and the wells were rinsed with PBS 2-3 times to remove residual medium. Subsequently, 100 μl serum-free DMEM/F12 was added to each well with 10 μl CCK-8 to assess cell viability. The plates were then returned to the cell culture incubator for 2 h, optical density (OD) at 450 nm was measured using a microplate reader and the absorbance values for each well were recorded.

Toluidine blue staining. Toluidine blue staining was used to stain cartilage and chondrocytes (25). Chondrocytes were seeded in 12-well plates with pre-laid coverslips ($8x10^4$/well; confluence of approximately 60%) and then removed and rinsed with PBS buffer three times. The cells were then fixed with 4% paraformaldehyde for 20 min at 4˚C and washed with distilled water three times. Subsequently, toluidine blue chondrocyte staining solution was added for 30 min at 37˚C, cells were washed with distilled water three times and water was drained using filter paper. Subsequently, cells were differentiated with 100% acetone (room temperature, 30 sec) until the chondrocytes were blue-purple and distinguishable, dehydrated with gradient ethanol, immersed in xylene and sealed with neutral gum to dry before observation under a light microscope.

Western blotting. A total of $3x10^5$ chondrocytes were grown in 6-well plates and treated with LPS (1 μg/ml), nicotinamide (10 mM) (26) and SAL (5 and 10 μm) for 24 h at 37˚C. Cells were washed with PBS 2-3 times and lysed with an 80ulRIPA lysis buffer and PMSF (100:1) per well. The lysed samples were placed on ice in a shaker for 20 min followed by centrifugation for 15 min (13,700 x g/min; 4˚C). The supernatant was collected, and the protein concentration was determined using a BCA protein concentration assay kit. Protein samples (10 μg/lane) was loaded onto 10% pre-made polyacrylamide gels for electrophoresis (100 V for 50 min). The proteins were transferred to the PVDF membrane (240 A for 90 min). PVDF membrane was cut into strips of corresponding molecular mass, and the membrane was incubated with rapid Blocking Buffer (Beyotime Institute of Biotechnology; cat. no. P0252) for 15 min at room temperature; after washing the membrane three times with TBST (containing 0.1% Tween 20), the strips were placed in primary antibody incubation solution [Col2; Mmp3; Mmp13; Bax; Bcl2; Gpx4; Slc7a11; Sirt1; FoxO1; phosphorylated (p-) FoxO1(Affinity, cat. no. AF3416). All antibodies are at a 1:1,000 dilution.] at 4˚C overnight. Following washing three times with TBST, the strips were placed in diluted secondary antibody (1:5,000) incubation solution for 1.5 h at room temperature on a shaker; the strips were washed three times with TBST and exposed in a dark room by placing the strips on an exposure cassette, adding developer solution dropwise (1:1 AB solution). Membranes were placed in the Bio-Rad imaging system for exposure. The exposed strips were scanned by a gel imaging system (Bio-Rad Laboratories, Inc.) and processed by ImageJ (National Institutes of Health, V.1.8.0-172), semi-quantified by western blot grayscale scanning and analyzed by GraphPad Prism software (Dotmatics, version 9.0.2).

Determination of ROS and lipid ROS levels. Intracellular levels of ROS and lipid peroxides were assessed using ROS (Biosharp Life Sciences, cat. no. BL714A) and lipid peroxides assay kits (Beyotime Institute of Biotechnology; cat. no. S0043M). Following treatment with LPS (1 μg/ml) and SAL (5 and 10 μm) for 24 h at 37˚C, chondrocytes were washed with PBS to remove residual media. DCFH-DA probe at a final concentration of 10 μM or BODIPY C11 probe at a concentration of 2 μM was added at 37˚C in the dark for 30 min to allow the probe to penetrate and be converted to fluorescent form in the presence of ROS and lipid peroxides, and the cells were washed twice with PBS. The cells were observed under a fluorescence microscope and images were captured to visualize intracellular oxides.

GSH detection assay. Cells were seeded into 6-well plates ($1x10^6$ chondrocytes), collected and washed twice with PBS; reagent 1 (cat. no. BC1175; Beijing Solarbio, and the kit was used according to the manufacturer's instructions) was added to the suspended cells and the cells were placed in liquid nitrogen at -80˚C followed by immersion in a water bath at 37˚C to freeze and thaw three times, each time for 3 min. Cells were centrifuged with a high-speed centrifuge (8,000 x g; 10 min) at 4˚C, supernatant was collected and reagent 2 was placed in a water bath at 37˚C for 35 min. The standard curve was prepared according to the glutathione content assay kit (GSH,

cat. no. BC1175) using Reagent 1. Blank (20 distilled water; 140 Reagent 2; 40 μl Reagent 3), sample (20 sample; 140 Reagent 2; 40 μl Reagent 3) and standard curve wells (20 standard; 140 Reagent 2; 40 μl Reagent 3; three replicates/group) were mixed, and then the absorbance was measured at 412 nm at ambient temperature. The concentration of the samples was calculated according to the standard curve formula, and the GSH content was calculated.

MDA detection assay. Cells were seeded ($1x10^6$ chondrocytes), the cells by adding 1 ml lysis buffer from the MDA content assay kit at room temperature and shaking, centrifuged (8,000 x g, 10 min, 4˚C) and placed the supernatant on ice. In the experimental group, 300 MDA working solution, 100 distilled water and 100 μl MDA kit reagent 3 were added to each tube. In the control group, 300 MDA working solution and 100 μl MDA kit reagent 3 were added. The mixture was incubated in a water bath at 100˚C for 2 h and cooled immediately on ice. The mixture was then centrifuged (1,000 x g; 10 min; room temperature) and 200 μl supernatant was placed in a 96-well plate; absorbance value at 532 nm was tested with enzyme-labeling apparatus. The amount of MDA was calculated according to the manufacturer's instructions.

Transmission electron microscopy. After treating the cells with LPS (1 μg/ml) and SAL (5 and 10 μm) for 24 h at 37˚C, the cells were fixed with 2.5% glutaraldehyde solution at 4˚C overnight. Cells were dehydrated stepwise with ascending ethanol and transferred to absolute acetone. Samples were embedded in epoxy resin and cut sections of 60 nm thickness. Sections were stained with 2% uranyl acetate solution for 30 min at room temperature, followed by staining in a 1% lead citrate solution for 5-8 min at room temperature. Samples were observed under a transmission electron microscope.

Statistical analysis. Results are from at least three different experiments. Data are presented as the mean ± SD. Data were analyzed using SPSS 25.0 software (IBM Corp.) and comparisons between multiple samples satisfying normal distribution were performed using one-way ANOVA and Tukey's post hoc test. $P<0.05$ was considered to indicate a statistically significant difference.

Results

Bioinformatics analysis of SAL and ferroptosis-associated targets in OA. A total of 512 targets for drug therapy were obtained by entering the chemical structure formula of SAL into Targenet, SwissTargetPrediction and Pharmmapper. GeneCards, DrugBank, and TTD databases were searched and 4,723 potential targets were obtained, combined with ferroptosis-associated targets and duplicate genes were removed, resulting in 34 intersecting targets (Fig. 1A). PPI networks were constructed for these potential targets to understand the functional interactions between cellular expression and proteins (Fig. 1B). Enrichment analysis of potential targets revealed their biological roles and pathways. These biological processes included 'cellular response to oxidative stress' (Fig. 1C). In addition, KEGG pathway enrichment analysis revealed that these targets were concentrated in biological pathways such as 'FoxO signaling pathway', 'lipid and atherosclerosis' and 'apoptosis' (Fig. 2A and B).

SAL increases viability of LPS-induced chondrocytes and protects extracellular matrix from degradation. To screen the optimal concentration of SAL for chondrocyte treatment, chondrocytes were treated with LPS and SAL (0-50 μM). Concentrations of 2.5-10.0 μM were significant at 24 h, whereas at 48 h only concentrations of 5 and 10 μM were significant. (Fig. 3A and B). Therefore, these concentrations were used for subsequent experiments. Toluidine blue staining of chondrocytes revealed light blue cytoplasm and dark blue nuclei. The number of chondrocytes was reduced, and the number of cellular projections were increased in the model group, whereas these phenomena were alleviated following SAL treatment (Fig. 3C). Subsequently, the therapeutic effect of SAL on LPS-induced chondrocyte apoptosis and extracellular matrix was verified using western blotting. Col2 expression decreased and Mmp3 and Mmp13 expression increased with LPS treatment. Similarly, Bax expression increased whilst Bcl2 expression decreased. These results suggested that LPS can induce chondrocyte apoptosis as well as extracellular matrix degradation. Additionally, SAL was largely able to reverse the effects induced by LPS, especially at high concentrations (Fig. 3D-I). These results suggested that SAL reversed the decrease in chondrocyte viability caused by LPS in a dose-dependent manner and protected cartilage extracellular matrix from degradation.

SAL attenuates LPS-induced ferroptosis in chondrocytes. As aforementioned lipid and oxidative stress are target pathways associated with ferroptosis. Therefore, LPS-induced ferroptosis in chondrocytes was investigated. Electron microscopy revealed that LPS-treated cells exhibited atrophied mitochondria, increased membrane density and no obvious DNA breaks in the nucleus, features of ferroptosis, which could be reversed by the SAL intervention (Fig. 4A). The ferroptosis marker proteins Gpx4 and SLC7A11 were detected using western blotting, which revealed that expression of these proteins decreased following LPS induction, while SAL treatment increased the expression of these proteins (Fig. 4B-D). LPS decreased GSH content in chondrocytes and increased the oxidative MDA content (Fig. 4E and F). These results verified that intracellular ferroptosis was occurring. Intracellular lipid peroxide and ROS content was detected with BODIPY C11 and DCFH-DA probe. The results suggested that LPS-induced chondrocytes had low levels of unoxidized lipids (red fluorescence) and high levels of oxidized lipids (green fluorescence.) SAL relieved intracellular lipid peroxidation stress, although not to the same level as the control group (Fig. 4G). Similar results were obtained by the intracellular ROS assay (Fig. 4H). These results demonstrated that SAL alleviated LPS-induced ferroptosis in chondrocytes.

SAL alleviates intracellular ferroptosis in chondrocytes by modulating the sirt/FoxO1 pathway. Network pharmacology analysis revealed that SAL may be involved in OA through the FoxO pathway. Western blotting revealed that intracellular sirt1 levels decreased in response to LPS induction, as did p-FoxO1 expression; expression of both increased following

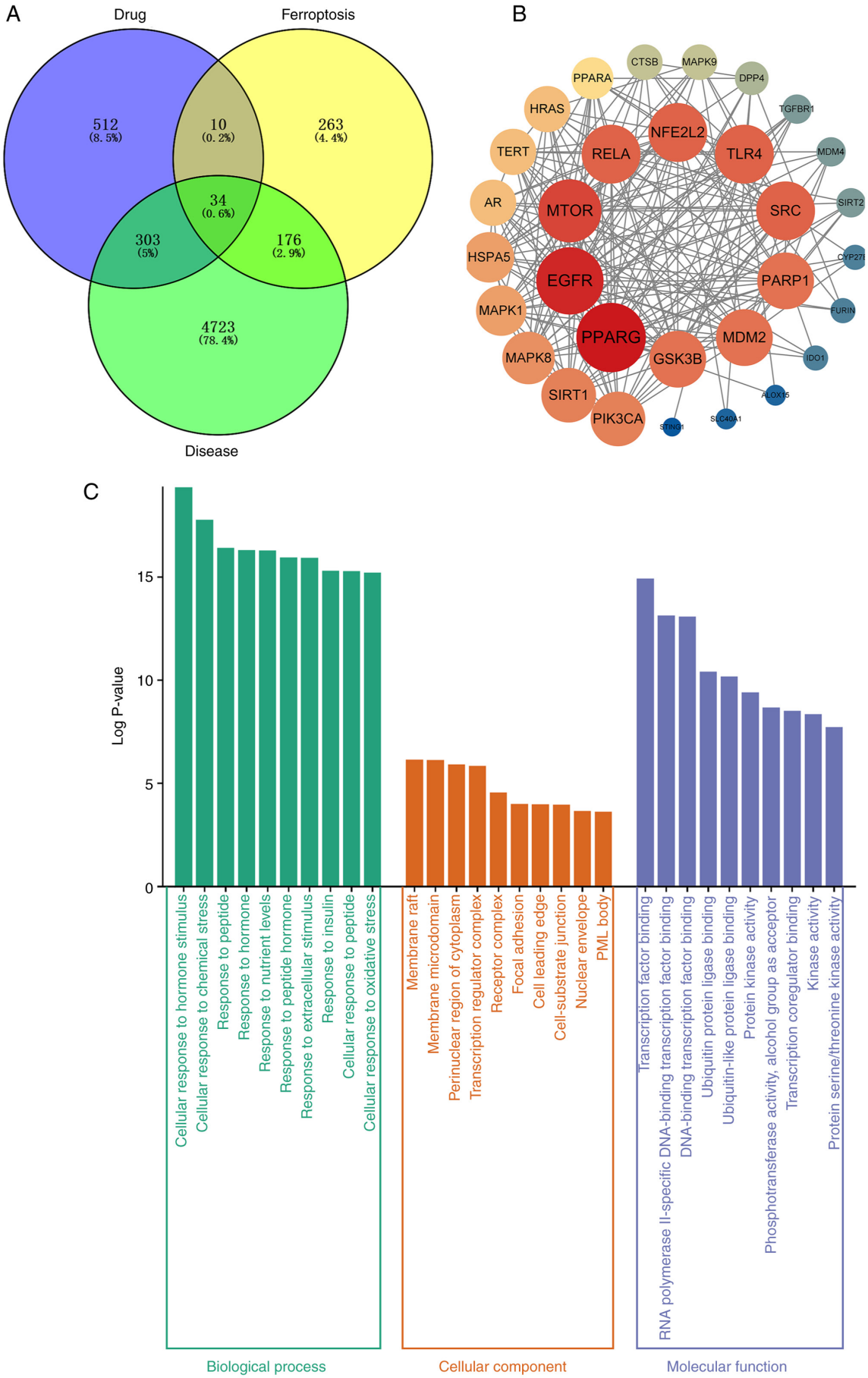

Figure 1. Target acquisition and enrichment analysis of SAL for ferroptosis in osteoarthritis. (A) Venn diagram of salidroside vs. OA target genes and ferroptosis targets. (B) PPI interaction network diagram of intersecting targets. (C) Biofunctional analysis of Gene Ontology for salidroside treatment of OA. OA, osteoarthritis; PPI, protein-protein interaction.

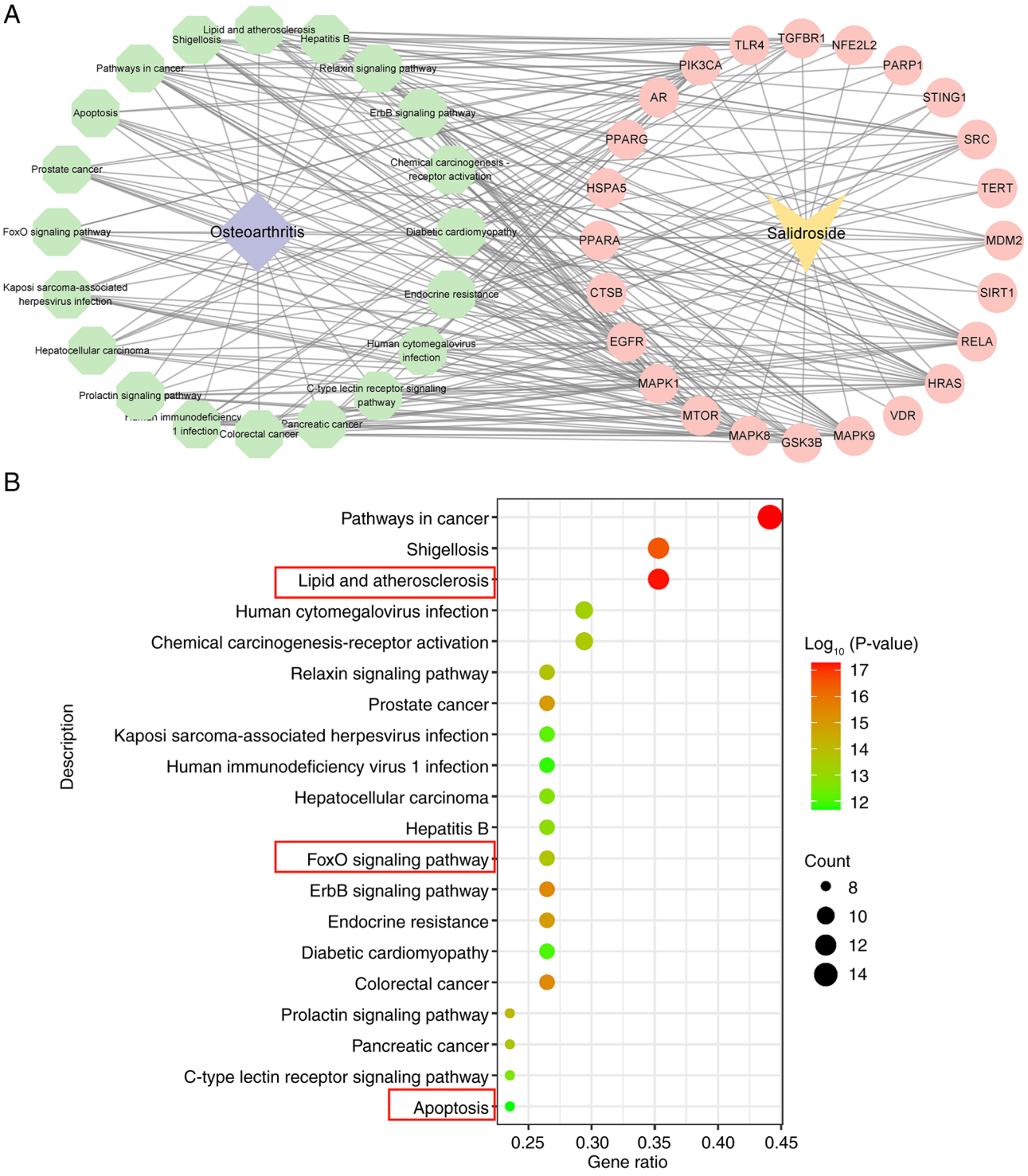

Figure 2. KEGG enrichment analysis of SAL targets for the treatment of ferroptosis in osteoarthritis. (A) Target-pathway network diagram of core targets. (B) Map of the top 20 signaling pathways for Kyoto Encyclopedia of Genes and Genomes.

SAL treatment, suggesting regulation of this pathway by SAL (Fig. 5A-C). SAL was docked to these two protein molecules, and both bound well (Fig. 5D). To validate the role of SAL in this pathway, the sirt1 inhibitor nicotinamide was used, which prevented the SAL-induced increase in sirt 1 and p-FoxO1 protein levels. Increased expression of both Gpx4 and SLC7A11 proteins was similarly inhibited (Fig. 5E-I). Therefore, SAL may regulate ferroptosis in chondrocytes by modulating the Sirt/FoxO1 pathway.

Discussion

OA is characterized by chondrocyte dedifferentiation and cartilage degeneration and defects. There is a lack of effective drugs to promote the repair of cartilage damage in patients with OA, and treatment is focused on delaying disease progression (27). Articular cartilage is primarily composed of chondrocytes, which produce extracellular matrix. Numerous factors such as inflammatory cytokines, abnormal mechanical

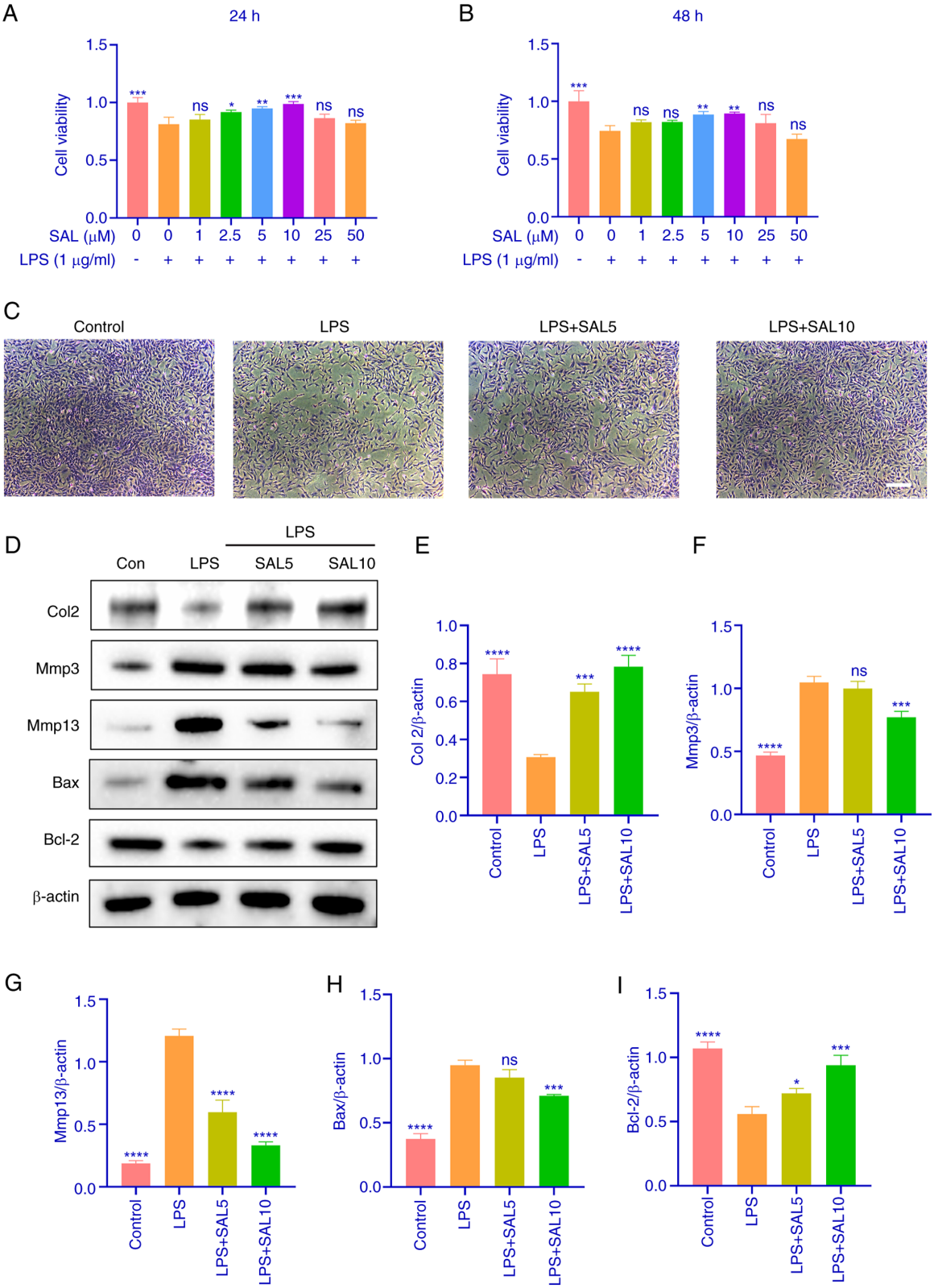

Figure 3. SAL increases viability of LPS-induced chondrocytes and protects extracellular matrix from degradation. Viability of chondrocytes following LPS and SAL treatment for (A) 24 and (B) 48 h. (C) Toluidine blue staining plots of chondrocytes after intervention with SAL and LPS for 24 h. Scale bar, 100 μm. (D) Representative western blot analysis of (E) Col2, (F) Mmp3, (G) Mmp13, (H) Bax, (I) Bcl-2. ****P<0.0001, ***P<0.001, **P<0.01, *P<0.05 vs. LPS (1 μg/ml) + 0 μM SAL. LPS, lipopolysaccharide; SAL, salidroside; Col2, Collagen II; ns, non-significant.

stimuli, chondrocyte cell demodulation and oxidative stress can disrupt the balance between chondrocyte physiology and matrix conversion, which can lead to matrix loss and tissue degeneration, thus leading to OA (28). There are two primary classes of drugs that induce OA in *in vitro* models, one belonging to cytokines and the other to endotoxins. Cytokines

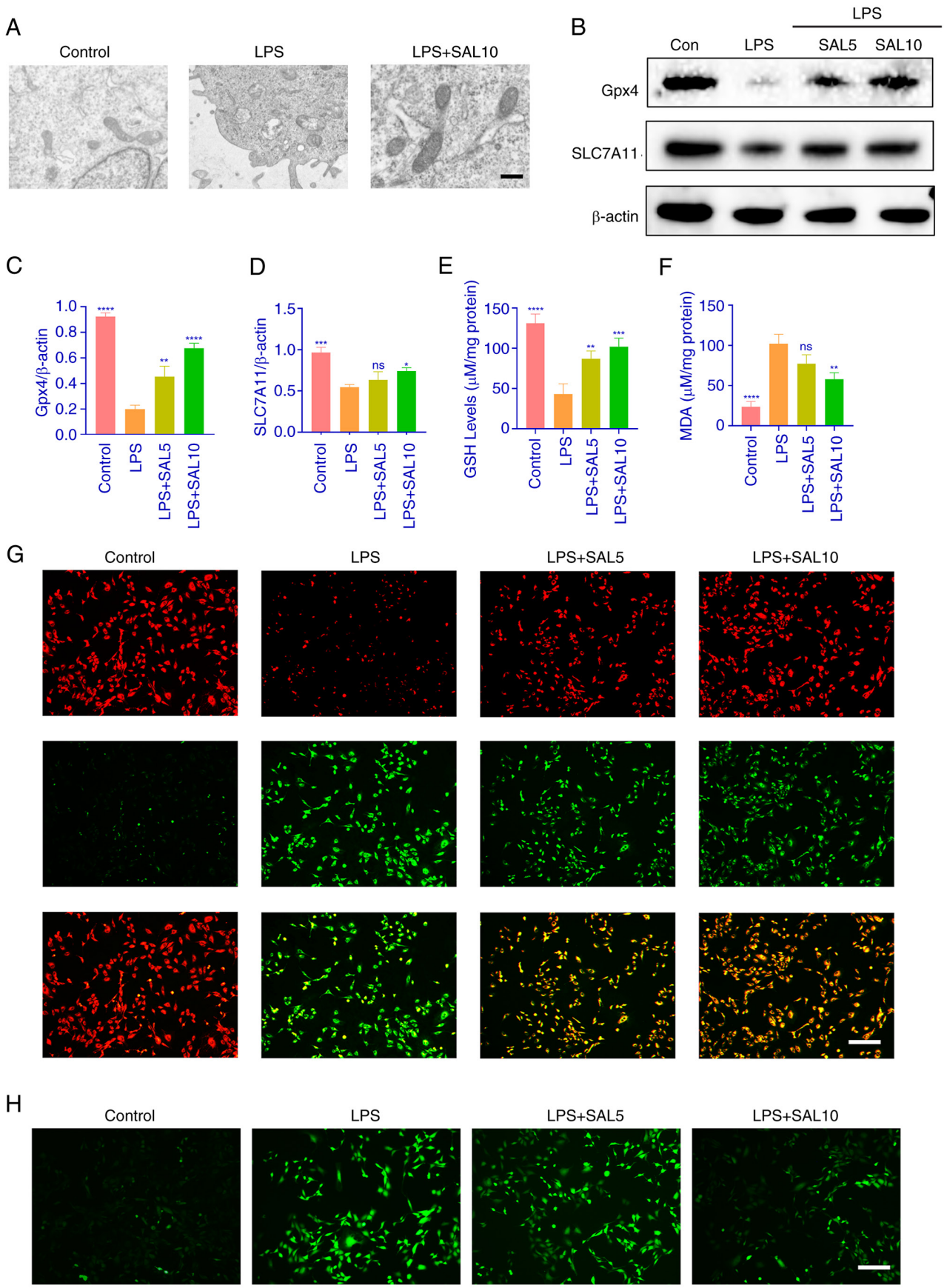

Figure 4. SAL attenuates LPS-induced ferroptosis in chondrocytes. (A) Electron microscopy was used to observe the morphology of chondrocytes following LPS and SAL treatment. Scale bar, 500 nm. (B) Representative western blot analysis of (C) Gpx4 and (D) SLC7A11. (E) GSH and (F) MDA content determination in chondrocytes. (G) BODIPY C11 probe incubation of chondrocytes to detect intracellular LPO fluorescence intensity. (H) DCFH-DA probe incubated chondrocytes to detect intracellular ROS fluorescence intensity. Scale bar, 100 μm. ****P<0.0001, ***P<0.001, **P<0.01, *P<0.05. vs. LPS. LPS, lipopolysaccharide; SAL, salidroside; ROS, reactive oxygen species; ns, non-significant; Gpx4 glutathione Peroxidase 4; SLC7A11, Solute Carrier Family 7 Member 11; GSH, Glutathione; MDA, Malondialdehyde; LPO, Lipid Reactive Oxygen Species.

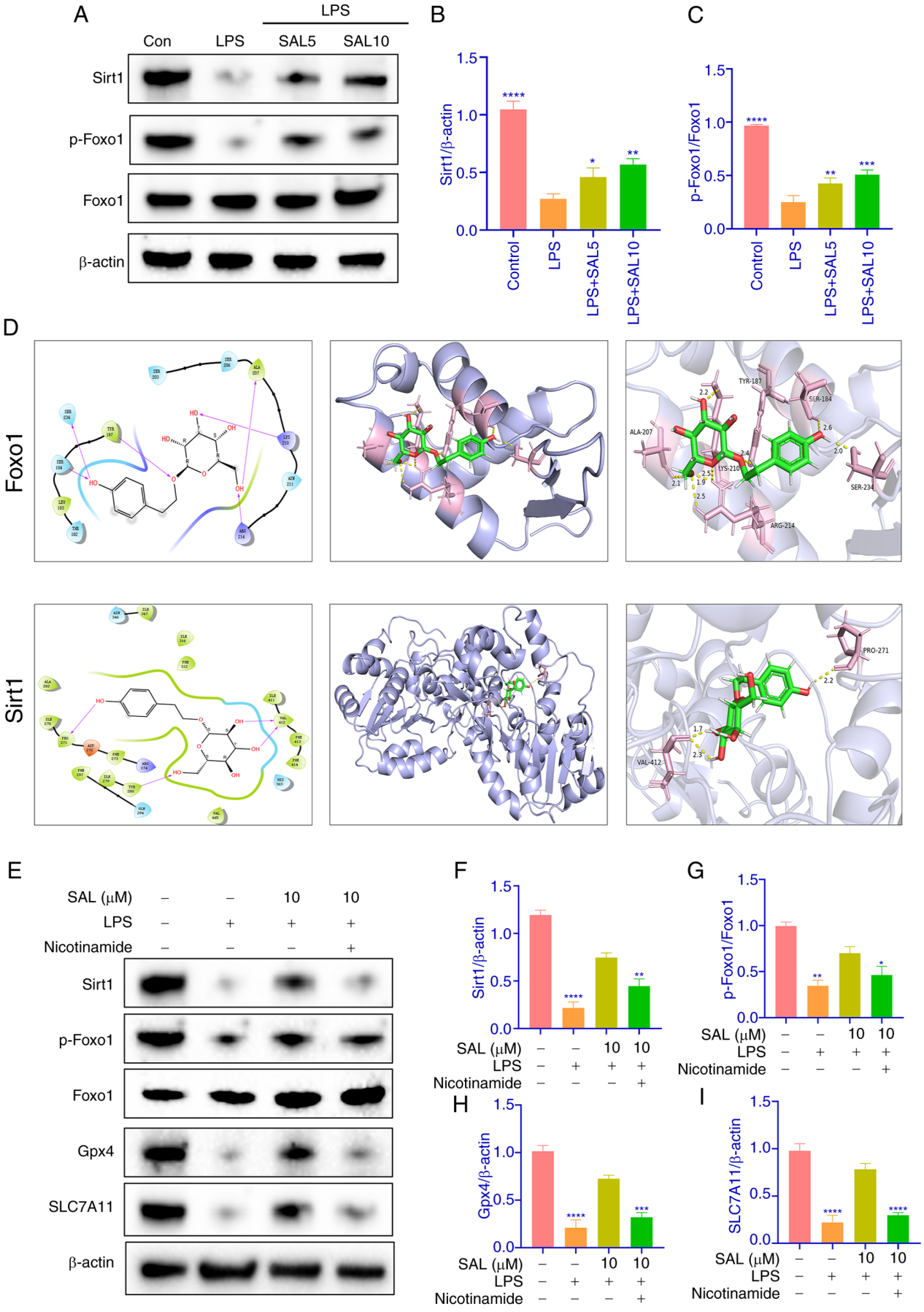

Figure 5. SAL alleviates intracellular ferroptosis in chondrocytes by modulating the sirt/FoxO1 pathway. (A) Representative western blots of (B) sirt1 and (C) p-FoxO1. (D) 2D and 3D molecular docking of SAL with Sirt1 and FoxO1. (E) Representative western blots of (F) sirt1, (G) p-FoxO1, (H) Gpx4 and (I) SLC7A11 following nicotinamide treatment. ****P<0.0001, ***P<0.001, **P<0.01, *P<0.05. vs. LPS. SAL, salidroside; LPS, lipopolysaccharide; sirt1, silent information regulator 1; p-FoxO1, phosphorylated Forkhead box protein O1; Gpx4, Glutathione Peroxidase 4; SLC7A11, Solute Carrier Family 7 Member 11.

are represented by IL1β and TNFα, and endotoxins are represented by LPS, which are used in the majority of *in vitro* models of OA (29-32). Therefore, LPS was selected for the *in vitro* model. In the present study, changes in chondrocytes were observed in an LPS-induced *in vitro* inflammation model. Number of chondrocytes in the model group was significantly decreased, the morphology was changed and the tentacles were increased. The western blotting showed a decrease in Col2 and Bcl2, and an increase in MMP3, MMP13, and Bax in the model group, indicating that the extracellular matrix of cartilage was damaged and the apoptotic index was increased. Following SAL intervention in the cells, the expression of Col2, MMP3, MMP13, Bcl2 and Bax were reversed. SAL not only increased the cell viability with increasing concentrations but also restored the extracellular matrix and apoptosis.

'FoxO signaling pathway', 'lipid and atherosclerosis' and 'apoptosis' were selected for analysis. Firstly, among the top 20 pathways, due to the large database and the overlapping nature of the pathways, there were pathways that were not relevant to the present study, such as 'pathways in cancer', 'Shigellosis', 'human cytomegalovirus infection', 'chemical carcinogenesis-receptor activation', 'relaxin signaling pathway', 'prostate cancer', 'Kaposi Sarcoma-associated herpesvirus infection', 'human immunodeficiency virus 1 infection', 'hepatocellular carcinoma' and 'hepatitis B'. Research on ferroptosis primarily focuses on oxidative stress and apoptosis; these two processes have interactions with each other (33,34). Lipid peroxidation is one of the key pathways to activate ferroptosis (35). Sirt1/FoxO1 signaling pathway is involved in oxidative stress (36), cellular regulation (37) and ferroptosis (7). In addition, targeting the sirt1/FoxO1 pathway regulates anti-inflammatory effects with the NF-κB pathway for the treatment of numerous types of diseases, including neurological, cardiovascular and digestive disease (38-40).

The sirt1/FoxO1 pathway not only interacts with the NF-κB pathway, but also with the PI3K/Akt pathway to regulate oxidative stress and apoptosis for the treatment of diabetic cardiomyopathy (37). Since bioinformatics findings did not involve these pathways, analysis centered on the Sirt1/FoxO1 pathway. Sirt1 protein and FOXO transcription factors serve important regulatory roles in physiological processes such as chondrocyte proliferation, maturation and matrix synthesis; activation of sirt1 inhibits chondrocyte apoptosis, attenuates oxidative stress damage and inhibits the progression of arthritis (41,42). The sirt1 agonist resveratrol inhibits chondrocyte apoptosis and cell death by modulating the Wnt/β-catenin pathway; resveratrol also inhibits chondrocyte apoptosis and extracellular matrix degradation via the regulation of the Wnt/β-catenin pathway and attenuates cartilage damage (43), which suggests regulating the sirt1/FoxO1 pathway may be an important mechanism for regulating ferroptosis in chondrocytes and thus treating OA. SAL promoted phosphorylation of FoxO1 and increased the sirt1 levels. Following addition of the sirt1 inhibitor, the expression of p-FoxO1, Gpx4, SLC7A11 decreased. This suggested that SAL regulated chondrocyte ferroptosis via modulation of the Sirt1/FoxO1 pathway, which may ameliorate joint inflammation.

Ferroptosis is an iron-dependent, non-regulatory form of regulated cell death caused by lipid peroxidation and results from an imbalance in the antioxidant and oxidative systems of the body (44). Ferroptosis is associated with inflammatory joint disease. Studies have shown that mechanical stimulation promotes ferroptosis in chondrocytes and thus OA (45,46). Previous studies have shown that systemic iron overload and elevated intracellular iron uptake induce and exacerbate OA in animal (guinea pig and mouse) models and that Ferrostatin-1 inhibits the progression of OA in mouse models (47-49). FTH1 is a component of ferritin; during ferroptosis, FTH1 regulates intracellular iron concentration in addition to iron uptake, transport and storage. FTH1 also regulates cellular ferroptosis by modulating ferritinophagy (50-52). Therefore, FTH1 is a key protein in ferroptosis. Liang *et al* (7) demonstrated that FoxO1 inhibits ferroptosis in cardiomyocytes by directly targeting FTH1 protein (7). The aforementioned studies suggest that the FoxO1 pathway has a notable impact on ferroptosis, warranting further investigation. Ferritin deposition may be a potential target for the treatment of arthritic injury and may be regulated by the FoxO1 pathway. The present study included FerrDb, and in combination with drug-disease targets, screened a total of 34 intersecting targets. Finally, the top 20 targets were analyzed. The final pathway enrichment analysis included 'lipid and atherosclerosis' and 'apoptosis'. Electron microscopy revealed that LPS-treated cells exhibited atrophied mitochondria, increased membrane density and no obvious DNA breaks in the nucleus, features of ferroptosis, which were reversed by SAL intervention. Decreased expression of Gpx4 and SLC7A11 and intracellular GSH content and increased MDA content in the model group confirmed the occurrence of ferroptosis in an *in vitro* model of LPS-induced inflammation, as well as an increase in lipid ROS and ROS content; these adverse effects were reversed by SAL. This suggested that SAL prevented ferroptosis in inflammatory chondrocytes.

Limitations of the present study include the lack of *in vivo* validation and validation of other relevant targets screened by bioinformatics analysis, such as NFE2L2, MAPK1, MAPK8, etc. Future work should include the use of *in vivo* drug infusion techniques.

To the best of our knowledge, the present study is the first to demonstrate the association between sirt1/FoxO1 and ferroptosis. The present study demonstrated that SAL treated LPS-induced decline in chondrocyte viability, decreased apoptosis and intracellular LPO and ROS content and alleviated intracellular ferroptosis in chondrocytes. These effects may be achieved by modulating the sirt1/FoxO1 pathway.

Acknowledgements

Not applicable.

Funding

No funding was received.

Availability of data and materials

The data generated in the present study may be requested from the corresponding author.

Authors' contributions

XZ conceived the study and wrote the manuscript. LH wrote the manuscript and performed experiments. XZ and LH confirm the authenticity of all the raw data. WF analyzed data. DX collected data and performed bioinformatics analysis. YZ conceived the study and edited the manuscript. All authors have read and approved the final manuscript.

Ethics approval and consent to participate

This animal experiment was approved by the Animal Ethics Committee of the First Affiliated Hospital of Guangzhou University of Traditional Chinese Medicine (approval no. GZTCMF1-20240301-3).

Patient consent for publication

Not applicable.

Competing interests

The authors declare that they have no competing interests.

References

1. Woolf AD and Pfleger B: Burden of major musculoskeletal conditions. Bull World Health Organ 81: 646-656, 2003.
2. Hiligsmann M, Cooper C, Arden N, Boers M, Branco JC, Luisa Brandi M, Bruyère O, Guillemin F, Hochberg MC, Hunter DJ, *et al*: Health economics in the field of osteoarthritis: An expert's consensus paper from the European Society for Clinical and Economic Aspects of Osteoporosis and Osteoarthritis (ESCEO). Semin Arthritis Rheum 43: 303-313, 2013.
3. Ma J, Matkar S, He X and Hua X: FOXO family in regulating cancer and metabolism. Semin Cancer Biol 50: 32-41, 2018.
4. Akasaki Y, Hasegawa A, Saito M, Asahara H, Iwamoto Y and Lotz MK: Dysregulated FOXO transcription factors in articular cartilage in aging and osteoarthritis. Osteoarthritis Cartilage 22: 162-170, 2014.
5. Matsuzaki T, Alvarez-Garcia O, Mokuda S, Nagira K, Olmer M, Gamini R, Miyata K, Akasaki Y, Su AI, Asahara H and Lotz MK: FoxO transcription factors modulate autophagy and proteoglycan 4 in cartilage homeostasis and osteoarthritis. Sci Transl Med 10: eaan0746, 2018.
6. Mortuza R, Chen S, Feng B, Sen S and Chakrabarti S: High glucose induced alteration of SIRTs in endothelial cells causes rapid aging in a p300 and FOXO regulated pathway. PLoS One 8: e54514, 2013.
7. Liang C, Xing H, Wang C, Xu X, Hao Y and Qiu B: Resveratrol improves the progression of osteoarthritis by regulating the SIRT1-FoxO1 pathway-mediated cholesterol metabolism. Mediators Inflamm 2023: 2936236, 2023.
8. Liu H, Wang J, Yue G and Xu J: Placenta-derived mesenchymal stem cells protect against diabetic kidney disease by upregulating autophagy-mediated SIRT1/FOXO1 pathway. Ren Fail 46: 2303396, 2024.
9. Ren CZ, Wu ZT, Wang W, Tan X, Yang YH, Wang YK, Li ML and Wang WZ: SIRT1 exerts anti-hypertensive effect via FOXO1 activation in the rostral ventrolateral medulla. Free Radic Biol Med 188: 1-13, 2022.
10. Zhang S, Lu Y, Shi W, Ren Y, Xiao K, Chen W, Li L and Zhao J: SIRT1/FOXO1 axis-mediated hippocampal angiogenesis is involved in the antidepressant effect of chaihu shugan san. Drug Des Devel Ther 16: 2783-2801, 2022.
11. Ju J, Li XM, Zhao XM, Li FH, Wang SC, Wang K, Li RF, Zhou LY, Liang L, Wang Y, *et al*: Circular RNA FEACR inhibits ferroptosis and alleviates myocardial ischemia/reperfusion injury by interacting with NAMPT. J Biomed Sci 30: 45, 2023.
12. Zhou M, Liu YW, He YH, Zhang JY, Guo H, Wang H, Ren JK, Su YX, Yang T, Li JB, *et al*: FOXO1 reshapes neutrophils to aggravate acute brain damage and promote late depression after traumatic brain injury. Mil Med Res 11: 20, 2024.
13. Magani SKJ, Mupparthi SD, Gollapalli BP, Shukla D, Tiwari AK, Gorantala J, Yarla NS and Tantravahi S: Salidroside-Can it be a multifunctional drug? Curr Drug Metab 21: 512-524, 2020.
14. Wang C, Wang Q, Lou Y, Xu J, Feng Z, Chen Y, Tang Q, Zheng G, Zhang Z, Wu Y, *et al*: Salidroside attenuates neuroinflammation and improves functional recovery after spinal cord injury through microglia polarization regulation. J Cell Mol Med 22: 1148-1166, 2018.
15. Liu X, Zhou M, Dai Z, Luo S, Shi Y, He Z and Chen Y: Salidroside alleviates ulcerative colitis via inhibiting macrophage pyroptosis and repairing the dysbacteriosis-associated Th17/Treg imbalance. Phytother Res 37: 367-382, 2023.
16. Chen H, Zhu J, Le Y, Pan J, Liu Y, Liu Z, Wang C, Dou X and Lu D: Salidroside inhibits doxorubicin-induced cardiomyopathy by modulating a ferroptosis-dependent pathway. Phytomedicine 99: 153964, 2022.
17. Pu WL, Zhang MY, Bai RY, Sun LK, Li WH, Yu YL, Zhang Y, Song L, Wang ZX, Peng YF, *et al*: Anti-inflammatory effects of Rhodiola rosea L: A review. Biomed Pharmacother 121: 109552, 2020.
18. Gao H, Peng L, Li C, Ji Q and Li P: Salidroside alleviates cartilage degeneration through NF-κB pathway in osteoarthritis rats. Drug Des Devel Ther 14: 1445-1454, 2020.
19. Sa L, Wei X, Huang Q, Cai Y, Lu D, Mei R and Hu X: Contribution of salidroside to the relieve of symptom and sign in the early acute stage of osteoarthritis in rat model. J Ethnopharmacol 259: 112883, 2020.
20. Chen L, Zhang YH, Wang S, Zhang Y, Huang T and Cai YD: Prediction and analysis of essential genes using the enrichments of gene ontology and KEGG pathways. PLoS One 12: e0184129, 2017.
21. Chen L, Chu C, Lu J, Kong X, Huang T and Cai YD: Gene ontology and KEGG pathway enrichment analysis of a drug target-based classification system. PLoS One 10: e0126492, 2015.
22. Gosset M, Berenbaum F, Thirion S and Jacques C: Primary culture and phenotyping of murine chondrocytes. Nat Protoc 3: 1253-1260, 2008.
23. Zhang G, Huang C, Wang R, Guo J, Qin Y and Lv S: Chondroprotective effects of Apolipoprotein D in knee osteoarthritis mice through the PI3K/AKT/mTOR signaling pathway. Int Immunopharmacol 133: 112005, 2024.
24. Liu B, Lu Y, Wang Y, Ge L, Zhai N and Han J: A protocol for isolation and identification and comparative characterization of primary osteoblasts from mouse and rat calvaria. Cell Tissue Bank 20: 173-182, 2019.
25. Wang F, Xiao J, Li M, He Q, Wang X, Pan Z, Li S, Wang H, Zhou C: Picroside II suppresses chondrocyte pyroptosis through MAPK/NF-κB/NLRP3 signaling pathway alleviates osteoarthritis. PLoS One 19: e0308731, 2024.
26. Lee HI, Jang SY, Kang HT and Hwang ES: p53-, SIRT1-, and PARP-1-independent downregulation of p21WAF1 expression in nicotinamide-treated cells. Biochem Biophys Res Commun 368: 298-304, 2008.
27. Minnig MCC, Golightly YM and Nelson AE: Epidemiology of osteoarthritis: Literature update 2022-2023. Curr Opin Rheumatol 36: 108-112, 2024.
28. Berenbaum F, Wallace IJ, Lieberman DE and Felson DT: Modern-day environmental factors in the pathogenesis of osteoarthritis. Nat Rev Rheumatol 14: 674-681, 2018.
29. Chen W, Xiao J, Zhou Y, Liu W, Jian J, Yang J, Chen B, Ye Z, Liu J, Xu X, *et al*: Curcumenol regulates Histone H3K27me3 demethylases KDM6B affecting Succinic acid metabolism to alleviate cartilage degeneration in knee osteoarthritis. Phytomedicine 133: 155922, 2024.
30. Johnson CI, Argyle DJ and Clements DN: In vitro models for the study of osteoarthritis. Vet J 209: 40-49, 2016.
31. Li M, Xiao J, Chen B, Pan Z, Wang F, Chen W, He Q, Li J, Li S, Wang T, *et al*: Loganin inhibits the ROS-NLRP3-IL-1β axis by activating the NRF2/HO-1 pathway against osteoarthritis. Chin J Nat Med 22: 977-990, 2024.
32. Xiao J, Zhang G, Mai J, He Q, Chen W, Li J, Ma Y, Pan Z, Yang J, Li S, *et al*: Bioinformatics analysis combined with experimental validation to explore the mechanism of XianLing GuBao capsule against osteoarthritis. J Ethnopharmacol 294: 115292, 2022.
33. Jiang X, Stockwell BR and Conrad M: Ferroptosis: Mechanisms, biology and role in disease. Nat Rev Mol Cell Biol 22: 266-282, 2021.

34. Wang B, Wang Y, Zhang J, Hu C, Jiang J, Li Y and Peng Z: ROS-induced lipid peroxidation modulates cell death outcome: Mechanisms behind apoptosis, autophagy, and ferroptosis. Arch Toxicol 97: 1439-1451, 2023.
35. Dixon SJ and Olzmann JA: The cell biology of ferroptosis. Nat Rev Mol Cell Biol 25: 424-442, 2024.
36. Chen X, Han D, Liu T, Huang C, Hu Z, Tan X and Wu S: Asiatic acid improves high-fat-diet-induced osteoporosis in mice via regulating SIRT1/FOXO1 signaling and inhibiting oxidative stress. Histol Histopathol 37: 769-777, 2022.
37. Ren BC, Zhang YF, Liu SS, Cheng XJ, Yang X, Cui XG, Zhao XR, Zhao H, Hao MF, Li MD, *et al*: Curcumin alleviates oxidative stress and inhibits apoptosis in diabetic cardiomyopathy via Sirt1-Foxo1 and PI3K-Akt signalling pathways. J Cell Mol Med 24: 12355-12367, 2020.
38. Song H, Ding Z, Chen J, Chen T, Wang T and Huang J: The AMPK-SIRT1-FoxO1-NF-κB signaling pathway participates in hesperetin-mediated neuroprotective effects against traumatic brain injury via the NLRP3 inflammasome. Immunopharmacol Immunotoxicol 44: 970-983, 2022.
39. Song S, Chu L, Liang H, Chen J, Liang J, Huang Z, Zhang B and Chen X: Protective effects of dioscin against doxorubicin-induced hepatotoxicity via regulation of Sirt1/FOXO1/NF-κb signal. Front Pharmacol 10: 1030, 2019.
40. Tan Y, Bie YL, Chen L, Zhao YH, Song L, Miao LN, Yu YQ, Chai H, Ma XJ and Shi DZ: Lingbao huxin pill alleviates apoptosis and inflammation at infarct border zone through SIRT1-Mediated FOXO1 and NF-κ B pathways in rat model of acute myocardial infarction. Chin J Integr Med 28: 330-338, 2022.
41. Almeida M and Porter RM: Sirtuins and FoxOs in osteoporosis and osteoarthritis. Bone 121: 284-292, 2019.
42. Liu J, He X, Zhen P, Chen H, Zhou S, Tian Q, Wang R and Li X: Sirtuin type 1 signaling pathway mediates the effect of diosgenin on chondrocyte metabolisms in osteoarthritis. Zhong Nan Da Xue Xue Bao Yi Xue Ban 42: 121-127, 2017 (In Chinese).
43. Liu S, Yang H, Hu B and Zhang M: Sirt1 regulates apoptosis and extracellular matrix degradation in resveratrol-treated osteoarthritis chondrocytes via the Wnt/β-catenin signaling pathways. Exp Ther Med 14: 5057-5062, 2017.
44. Sun Y, Chen P, Zhai B, Zhang M, Xiang Y, Fang J, Xu S, Gao Y, Chen X, Sui X and Li G: The emerging role of ferroptosis in inflammation. Biomed Pharmacother 127: 110108, 2020.
45. Wang S, Li W, Zhang P, Wang Z, Ma X, Liu C, Vasilev K, Zhang L, Zhou X, Liu L, *et al*: Mechanical overloading induces GPX4-regulated chondrocyte ferroptosis in osteoarthritis via Piezo1 channel facilitated calcium influx. J Adv Res 41: 63-75, 2022.
46. Han J, Zhan LN, Huang Y, Guo S, Zhou X, Kapilevich L, Wang Z, Ning K, Sun M and Zhang XA: Moderate mechanical stress suppresses chondrocyte ferroptosis in osteoarthritis by regulating NF-κB p65/GPX4 signaling pathway. Sci Rep 14: 5078, 2024.
47. Burton LH, Radakovich LB, Marolf AJ and Santangelo KS: Systemic iron overload exacerbates osteoarthritis in the strain 13 guinea pig. Osteoarthritis Cartilage 28: 1265-1275, 2020.
48. Jing X, Lin J, Du T, Jiang Z, Li T, Wang G, Liu X, Cui X and Sun K: Iron overload is associated with accelerated progression of osteoarthritis: The role of DMT1 mediated iron homeostasis. Front Cell Dev Biol 8: 594509, 2021.
49. Simão M, Gavaia PJ, Camacho A, Porto G, Pinto IJ, Ea HK and Cancela ML: Intracellular iron uptake is favored in Hfe-KO mouse primary chondrocytes mimicking an osteoarthritis-related phenotype. Biofactors 45: 583-597, 2019.
50. Fang Y, Chen X, Tan Q, Zhou H, Xu J and Gu Q: Inhibiting ferroptosis through disrupting the NCOA4-FTH1 interaction: A new mechanism of action. ACS Cent Sci 7: 980-989, 2021.
51. Kong N, Chen X, Feng J, Duan T, Liu S, Sun X, Chen P, Pan T, Yan L, Jin T, *et al*: Baicalin induces ferroptosis in bladder cancer cells by downregulating FTH1. Acta Pharm Sin B 11: 4045-4054, 2021.
52. Tian Y, Lu J, Hao X, Li H, Zhang G, Liu X, Li X, Zhao C, Kuang W, Chen D and Zhu M: FTH1 inhibits ferroptosis through ferritinophagy in the 6-OHDA Model of Parkinson's disease. Neurotherapeutics 17: 1796-1812, 2020.